AIST-NT
Advanced Integrated Scanning Tools for Nano-Technology

TERS at Work: Identification of Mixed Carbon Species with 7nm Resolution

Sergey A. Saunin, Dmitry A. Evplov, Vasily V. Gavrilyuk, Andrey V. Krayev.

AIST-NT Inc, 359 Bel Marin Keys Blvd, Suite 20, Novato , CA, 94949

Tel: 1-415-884-9500, Fax: 1-415-884-2775, contact e-mail: akrayev@aist-nt.com

KEYWORDS:TERS, Raman Spectroscopy, Graphene, CNT, AFM, SPM

Introduction

For many years, tip enhanced Raman scattering (TERS), a hybrid method combining the advantages of scanning probe microscopy (SPM) and surface enhanced Raman scattering (SERS) was pursued in a very limited number of groups around the world. As it is the case with many novel techniques, the early TERS experiments were mainly conducted on self-built equipment [1,2] or extensively-modified commercial instruments. Two reasons for the limited spread of TERS research were the significant technical challenges of co-localization of reasonably high numerical aperture excitation / collection optics with the apex of the SPM tip and the lack of commercially available probes that could provide a strongly-enhanced Raman signal in a reproducible manner.

The rewards promised by TERS, though, would certainly justify the effort; this technique can fulfill the ultimate dream of analytical chemists –imaging of a single molecule in real space combined with its spectroscopic identification. Recently two independent groups[3,4] demonstrated this capability of the single-molecule TERS operating in Scanning Tunneling microscopy (STM) mode in ultrahigh vacuum at cryogenic temperatures. Hopefully these publication will serve as a catalyst for TERS-related research, similar to what the publications of Katrin Kneipp and Shoomin Nie [5,6] did for SERS.

Thanks to the efforts of the pioneers of TERS, today the technique is ready for broader distribution not just as an object of research in itself, but as a nanoscale analytical method. In recent years, significant progress has been made in high yield manufacturing of reliable TERS – active tips [7-10]. It is important to note that different groups developed significantly different approaches, this variety being of great importance for allowing TERS to address a larger range of real-world samples.

AIST-NTInc.has addressed the demand from the scientific community by developing a next-generation SPM, designed from the beginning to be integrated with Raman spectroscopy. Innovations dictated by the integration of the SPM with Raman spectroscopy like the 1300nm feedback laser, automated alignment of the laser-to-probe-to-photodiode, automated configuration of the feedback bandwidth and gains for the scanning etc., not only brought the performance of the integrated AFM-Raman system to a new level, but also greatly improved the convenience and ease of use of the SPM operations themselves.

AIST-NT's OmegaScope–R designed for TERS measurements of non-transparent samples allows high numeric aperture (0.7NA) access to the AFM cantilever from the top or the side, the

latter being the preferred configuration. The highest in industry numerical aperture from the side increases the efficiency of both the excitation and of the collection of scattered light. A unique closed-loop flexure-based objective scanner ensures nanometer-precision and long-term stability of the focus and alignment of the excitation laser with the apex of the SPM tip.

Advanced scanning procedures specifically developed by AIST-NT for TERS imaging complement efficient design of the integrated system and bring TERS performance to a new level. The fast mapping procedure, Swift Mode, developed in close collaboration with Horiba Scientific, allows mapping time to be drastically reduced and brings the overall performance of the system to the level at which it can be efficiently used as an analytical tool.

Fig.1 OmegaScope-R coupled with the Horiba XploRAupright Raman spectrometer

Carbon nanotubes (CNT), graphene and its derivatives have been extensively investigated using Raman spectroscopy. These materials are under consideration as replacements for silicon in

future electronic device and their characterization at the nanometer scale is thus of great importance. Since their Raman spectra are quite sensitive to even small variations in their structure, TERS is a very promising technique for the characterization of these materials on the nanometer scale.

Results and discussion

We chose for our experiments single wall carbon nanotubes and graphene oxide, co-deposited on gold-coated glass slides. These two carbon materials have significantly different morphology and also a clear difference in their Raman spectra: graphene oxide features intense, broad D and G bands while carbon nanotubes, as well as an intense G band, also feature RMB and 2D bands, absent in graphene oxide. Therefore, TERS mapping can be performed based on both the G band common for both materials, and on the D or 2D bands that define the chemical identity of these two species. A gold-coated substrate was chosen in order to implement gap-mode TERS, in which plasmonic electric filed excited in the probe is significantly confined within the gap between the apex of the probe and the substrate, thus improving the intensity and the spatial resolution of TERS signal.

TERS maps were collected using a side illumination scheme through a 100X 0.7 NA objective with vertically polarized red (638 nm) laser, Fig.2.

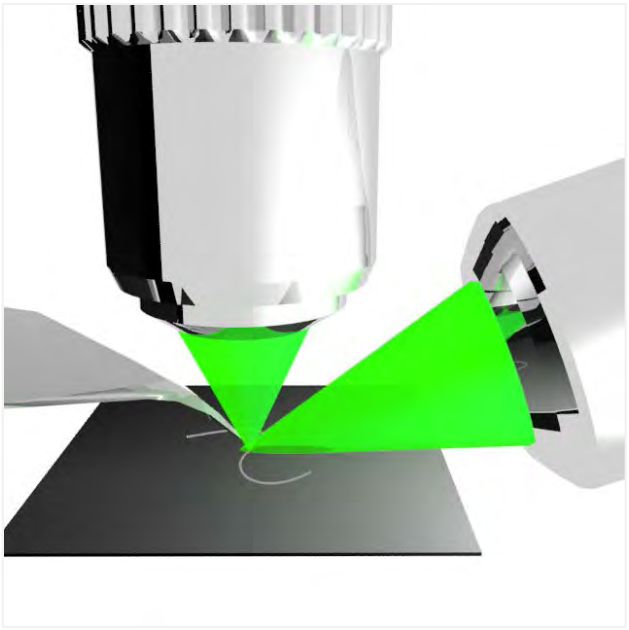

Fig.2 Illumination scheme used in experiments: excitation via side 100x, 0.7NA objective; video monitoring of sample and tip via top 10x, 0.28NA objective

This scheme provides the most straightforward approach to arranging significant Z polarization of the excitation beam and efficient collection of the scattered light. Two types of TERS probes were used:

- etched gold wire attached to a tuning fork operating in normal-force non-contact mode, and
- solid gold AFM cantilever with electrochemically etched tip (courtesy of Dr. Raul Rodriguez, Chemnitz University of Technology)

TERS results obtained in Tuning Fork operation mode

Typical TERS maps of an area of the sample are presented in Fig.3 along with corresponding topography and representative spectra.

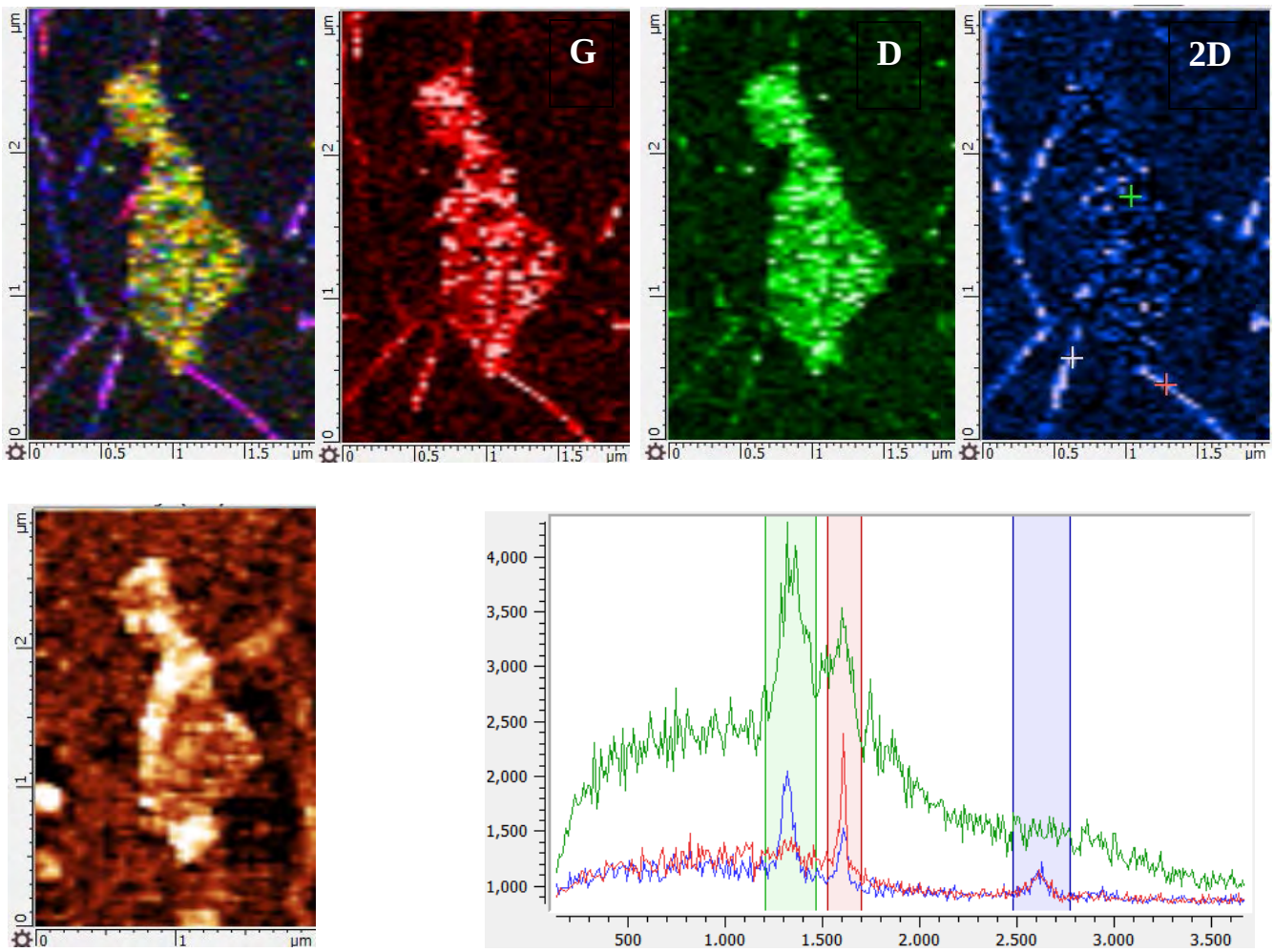

Fig.32 x 3µm TERS maps of graphene oxide/CNTs co-deposited on a gold-coated glass slide. Combined TERS map, maps of G,D and 2D bands correspondingly, topography image of the same area and typical spectra. Excitation: 638nm laser, 210µW, integration time 0.2s

Graphene oxide shows broad D-band (1350cm^{-1}) and G-band (1600cm^{-1})peaks, while carbon nanotubes, having a much less defective structure compared to graphene oxide, also show a significant 2D-band peak (around 2600cm^{-1}). It is very interesting to note that not all the

nanotubes in this area are the same. Two nanotubes in the left lower corner feature significant D-band peaks, while the others give rise to only G and 2D bands.

That the CNTs are not visible in the topography image recorded concurrently with the TERS maps, is a rather unexpected result, which we attribute mainly to the relatively low resolution of the map (only 40x90 pixels), it is also possible that the nanotubes topography is concealed by residual surfactant, remaining on the surface even after several rinsing cycles with pure water. Also, CNTs tend to blend into the topography of the underlying gold which makes them even less accessible with relatively blunt TERS probe. A lower portion of the area in Fig.3 was re-scanned at higher resolution in order to try to resolve the nanotubes in topography channel and to check how stable the TERS signal is. Results of these measurements are presented in Fig.4.

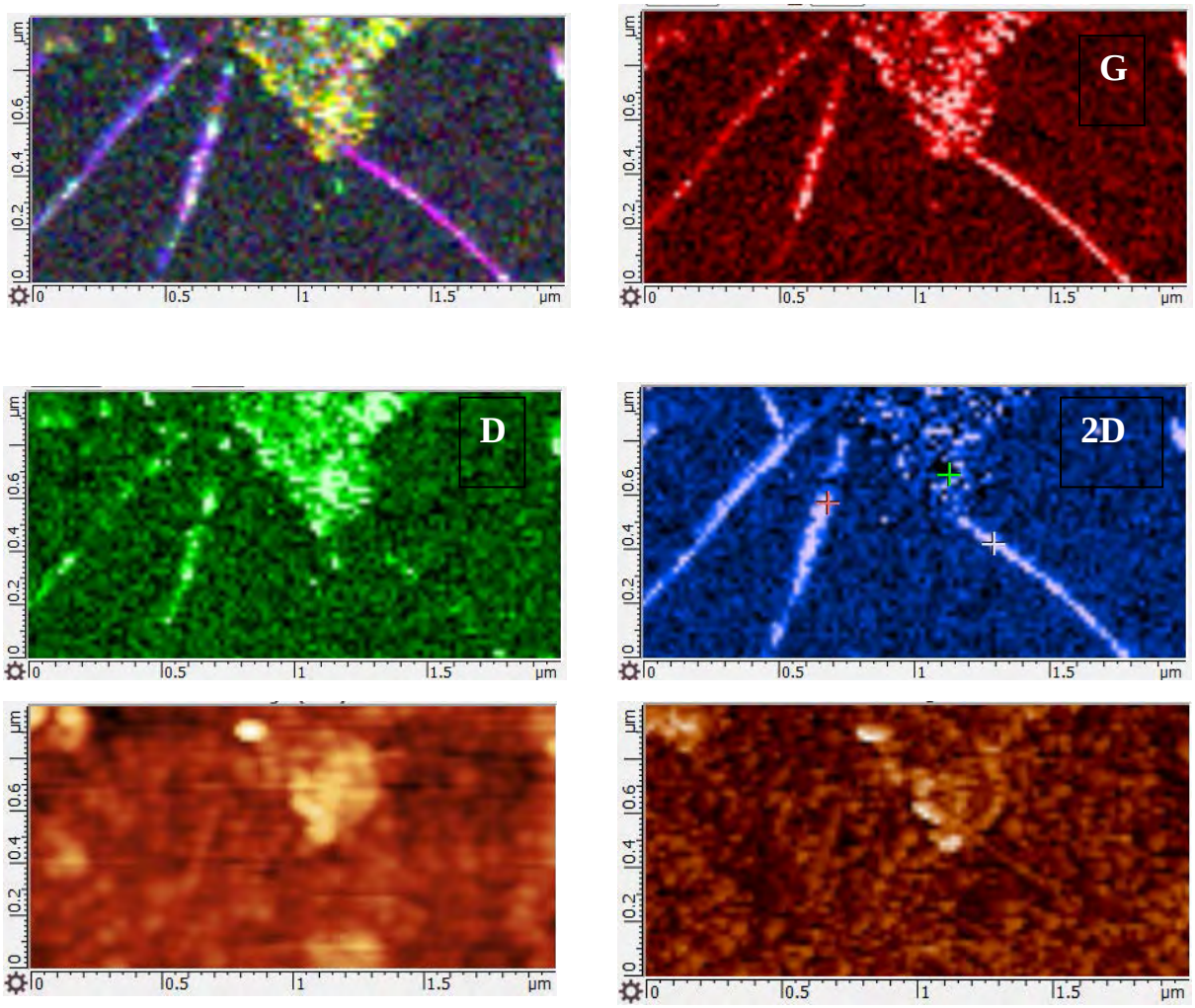

Fig.4 2x 1µm, 100x50 pixels TERS maps of lower portion of the CNTs and Graphene oxide flake from Fig.3. Combined TERS map, maps of G,D and 2D bands correspondingly, topography and dissipation mode images. Excitation: 638nm laser, 130µW, integration time 0.2s.

All spectral features observed in Fig.3 are also evident in the higher resolution image: the two nanotubes in the left lower corner demonstrate significant intensity of the D-band, while the nanotubes in the right lower corner are visible only in G-band and 2D-band maps. Due to the

higher resolution of the map, some of the nanotubes are now detected in the topography and the related amplitude (dissipation) channels.

The measurements presented in Fig.4 show a spatial resolution of about 30 nm, which is to great extent limited by the pixel size (20nm). In order to estimate the lateral resolution to be expected from this type of tip, we measured the TERS signal as a function of tip / surface separation. The tip was positioned over a graphene oxide flake and series of spectra taken at different tip / surface separations. The results, presented in Fig.5, show that the TERS signal decreases dramatically with extra lift from imaging position of only 3nm, making it reasonable to expect TERS XY resolution of about 5nm.

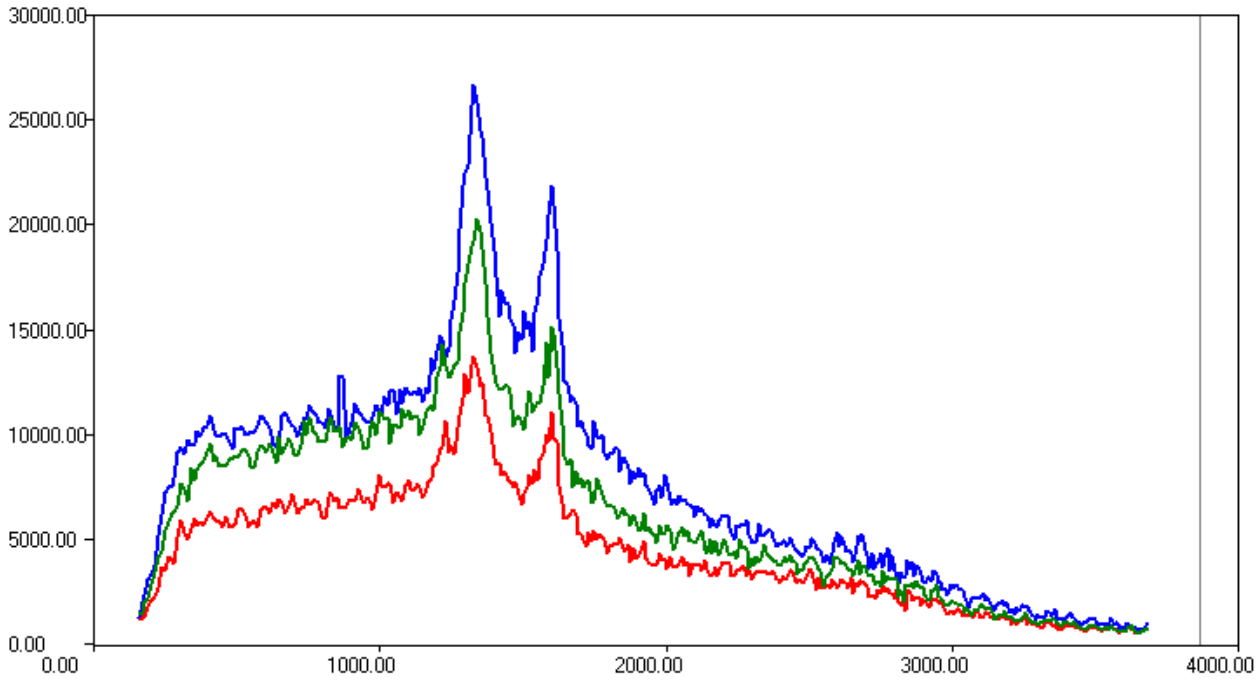

Fig.5 Dependence of the intensity of the TERS signal of graphene oxide on separation between the tip and sample. Blue curve: imaging position, green: 1nm lift, red: 2nm lift.

To confirm this estimate, TERS images of a another area on the same sample were taken with a pixel size of 15nm (Fig.6a) and of 3nm (Fig.6b).

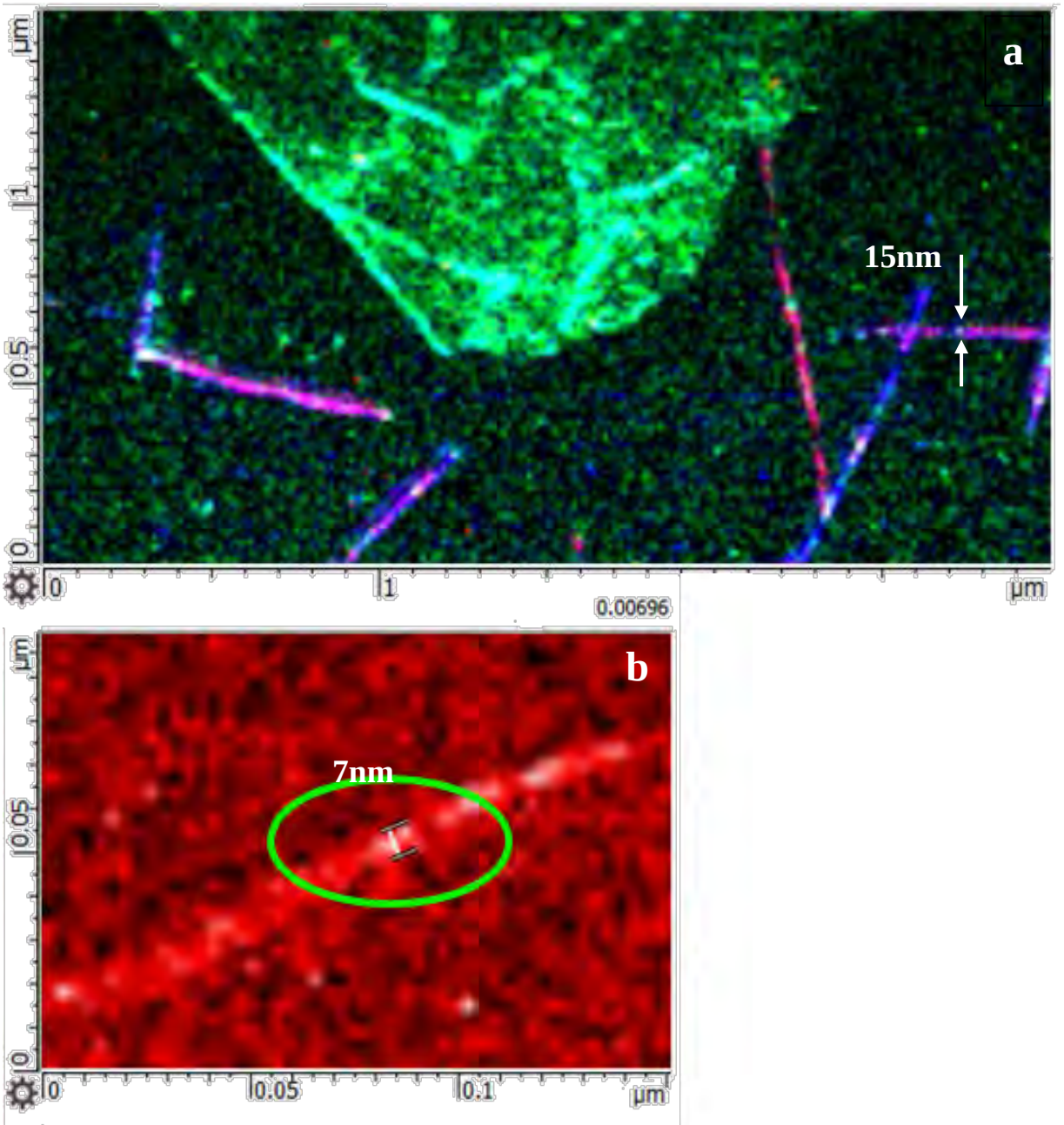

Fig.6 a):3x 1.5µm, 200x100 pixels Combined TERS map of the CNTs and Graphene oxide flake, pixel size limited resolution is 15nm. b): 150x 75nm TERS map of an individual SWCNT, resolution is about 7nm.

The spatial resolution achieved in the most successful measurement (Fig.6b) was about 7nm. We hope that this is not the ultimate limit and that spatial resolution can be further improved by the use of sharper tips and by further improving the accuracy of the scanning in normal-force tuning fork operation.

TERS results obtained in AFM operation mode

Solid gold etched AFM probes (courtesy of Dr. Raul Rodriguez, Chemnitz University) were used with the same excitation /collection optical layout as the tuning fork based probes: side access through a 100x, 0.7NA objective and video observation from above, through a 10x, 0.28NA objective. Two types of samples were used for AFM-based TERS measurements: the first type was identical to the graphene oxide/CNT sample co-deposited on gold, used for the tuning fork based TERS experiments. We also tried a slight variation of the first sample in which the gold surface was functionalized with a monolayer of organic molecules; which significantly increases the adhesion of graphene oxide.

In Fig.7, a combined TERS map of CNTs and graphene oxide deposited on a functionalized gold surface is presented, along with the typical spectra taken on graphene oxide, CNTs and on a bare area, with just linker molecules.

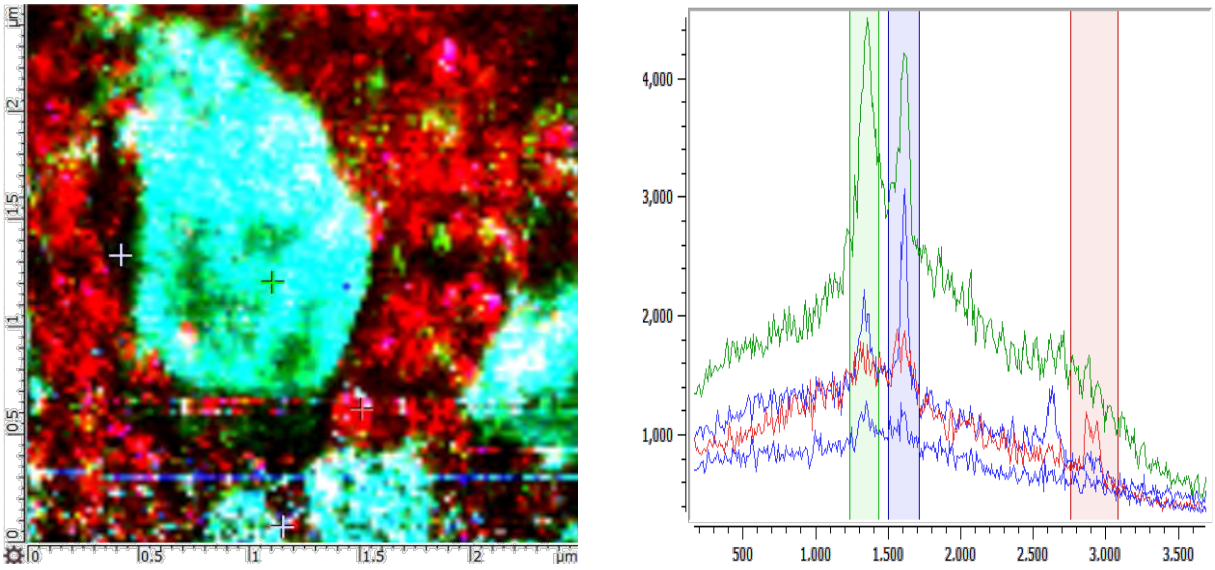

Fig.7 a) 2.5x2.5µm , 100 x100 pixels combined TERS map of the intensities of D, G and CH (2900cm^{-1}) bands. b) Typical spectra. Map was collected with a solid gold probe operating in AFM mode; 638nm laser, 210mW power, 300ms per pixel.

In Fig.8,a TERS map and related AFM data obtained on a sample in which the linker molecules were removed after deposition of graphene oxide and the CNTs are presented. The band at 2900cm^{-1}is absent in this map, confirming successful removal of the linker molecules. The tip used in this case demonstrated only moderate enhancement and, in order to keep the integration time at 100ms per pixel, the excitation power was increased to 2.1mW. As can be seen from the spectra in Fig.8d, it allowed signal-to noise ratio in the collected spectra to be maintained at a reasonably high level, allowing a high resolution map (128x128 pixels) to be completed in less than 30 minutes.

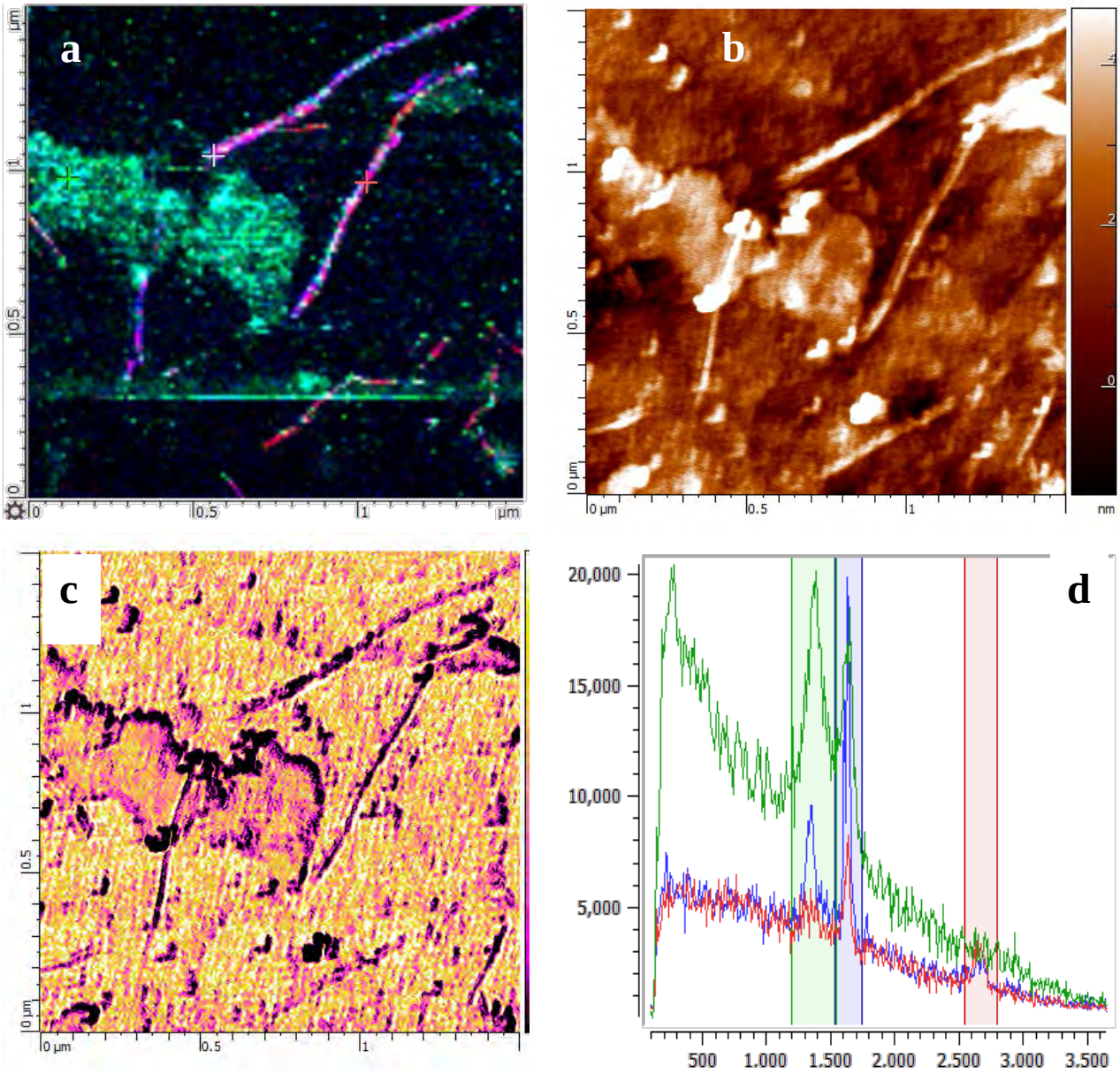

Fig.8 1.5 x 1.5μm a) 128 x 128 pixels combined TERS map of CNT/GO on gold. b) AFM topography and c) the phase shift of the same area, d) typical spectra; 638nm laser, 2.1mW, 100ms per pixel integration time.

It is important to note that some solid gold AFM probes produced extremely high enhancement which allowed either a reduction of the integration time to 20ms at 210μW excitation power or collection with a slightly longer integration time of 100ms but at power lever at the entrance of

the side objective of only 20µW. Both options may be of great importance for the high speed, high resolution imaging - where it is important to minimize drift - or for the TERS imaging of delicate samples that do not tolerate high intensity laser excitation.

Fast TERS measurements are presented in Fig.9. The sample used was identical to the sample used earlier for tuning fork-based TERS mapping, with no linker molecules used to attach the graphene oxide, as a result some areas lacked large flakes and featured mostly carbon nanotubes.

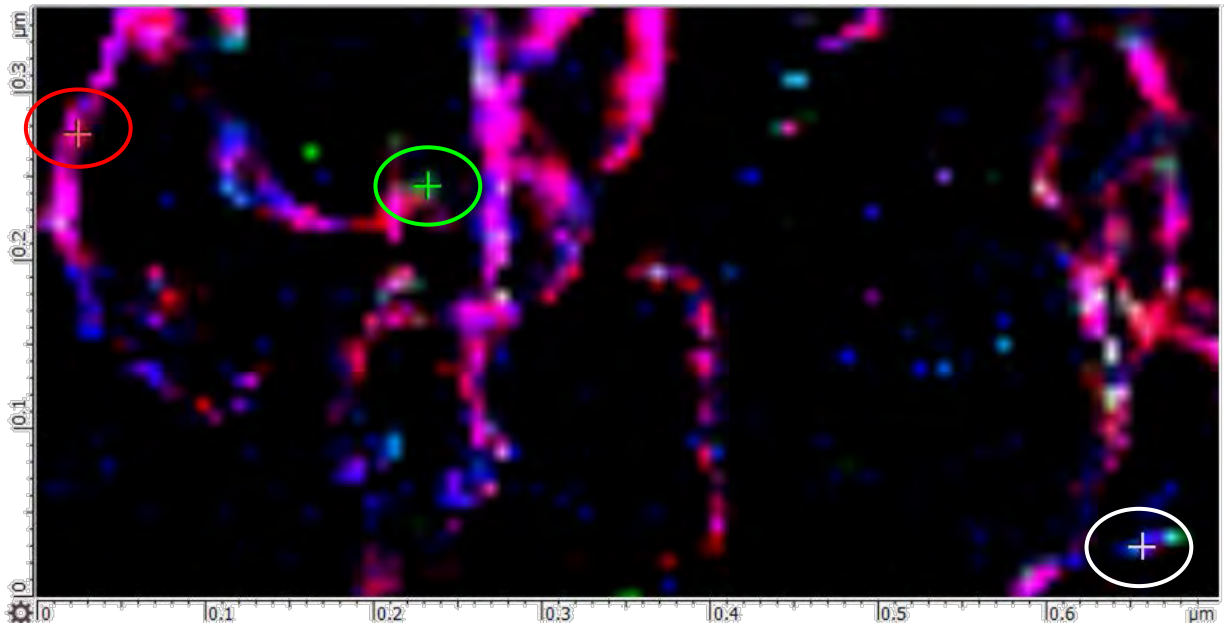

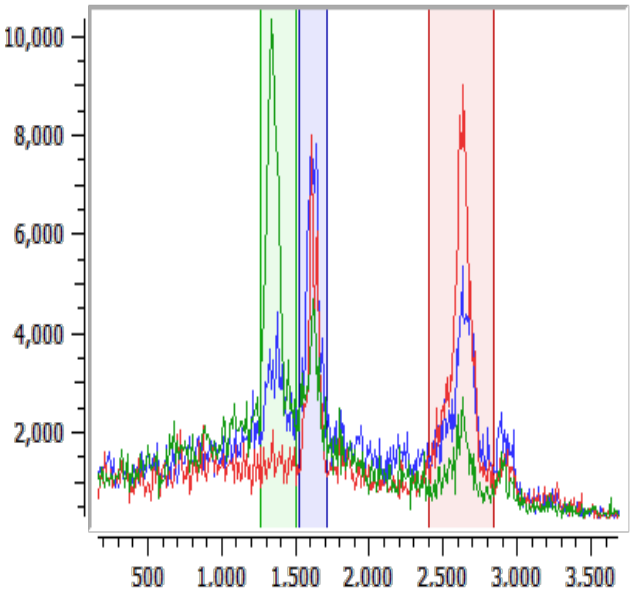

Fig.9 700 x 350nm, 100 x 50 pixels combined TERS map of CNTs and Graphene Oxide on gold. 638nm laser, 210µW, 20ms integration time. Typical spectra from marked locations. Note that the intensity of the 2D band in the TERS spectra is considerably higher compared to the far field. Image courtesy of Dr. Raul Rodriguez, Chemnitz University

Conclusions.

Due to significant innovations implemented in the AIST-NT OmegaScope-R, an integrated AFM-Raman system for non-transparent samples, its high optical efficiency and advanced TERS imaging scanning procedures, we successfully demonstrated simultaneous high resolution spatial and chemically-specific imaging of two different carbon species: single-walled carbon nanotubes and graphene oxide, co-deposited on gold. Not only were the two species of carbon unambiguously identified, based on their TERS spectra at a spatial resolution of 7nm, but we also found that the SWCNTs split into two groups, chemically; some showing significant D band intensity, while others featured only G and 2D bands.

The capability for high speed, high resolution TERS imaging has been demonstrated in both the Tuning-Fork and the AFM mode of operation.

Advances in the hardware and software development, implemented in the AIST-NT OmegaScope-R, allow routine high resolution TERS imaging of the carbon species,providing TERS capability as an analytical tool to a new level of performance and convenience.

Literature

1. Achim Hartschuh, Erik J. Sanchez, Sunney Xie and Lucas Novotny **Phys.Rev.Lett 90, 095503**
2. Bruno Pettinger, Bin Ren, Gennaro Picardi, Rolf Schuster, and Gerhard Ertl **Phys.Rev.Lett 92, 096101**
3. N. Jiang, E. T. Foley, J. M. Klingsporn, M. D. Sonntag, N. A. Valley, J. A. Dieringer, T. Seideman,G. C. Schatz, M. C. Hersam,*, and R. P. Van Duyne **Nano Letters 2012 12 (10), 5061-5067**
4. R. Zhang, Y. Zhang, Z. C. Dong, S. Jiang, C. Zhang, L. G. Chen, L. Zhang, Y. Liao, J. Aizpurua, Y. Luo, J. L. Yang & J. G.Hou **Nature Vol.498, 82-86**
5. Katrin Kneipp, Yang Wang, Harald Kneipp, Lev T. Perelman, Irving Itzkan, Ramachandra R. Dasari, and Michael S. Feld**Phys. Rev..Lett 78, 1667-1670**
6. Shuming Nie, Steven R. Emory **Science, Vol. 275 no. 5303 pp. 1102-1106**
7. Norihiko Hayazawa,Taka-aki Yano and Satoshi Kawata **J. Raman Spectrosc. 2012, 43, 1177–1182**
8. Bin Ren, Gennaro Piccardi and Bruno Pettinger**Rev. Sci. Instrum., Vol. 75, No. 4, 837-841**
9. Valentinas Snitka , Raul D. Rodrigues, Vitas Lendraitis**Microelectronic Engineering 88 (2011) 2759–2762**
10. Carlos A. Barrios, Andrey V. Malkovskiy, Alexander M. Kisliuk, Alexei P. Sokolov, and Mark D. Foster**J. Phys. Chem. C 2009, 113, 8158–8161**